16th World Conference on Earthquake, 16WCEE 2017

Santiago Chile, January 9th to 13th 2017

Paper N° 1206 (Abstract ID)

Registration Code: S-M1461846304

Interstory drift estimation of seismic-excited building structures using acceleration measurement

Jiazeng Shan [(1)], Yuting Ouyang [(2)], Weixing Shi [(3)]

[(1)] *Assistant professor, Research Institute of Structural Engineering and Disaster Reduction, Tongji University, Shanghai, China, 200092, E-mail: 08jzshan@tongji.edu.cn*
[(2)] *Graduate student, Research Institute of Structural Engineering and Disaster Reduction, Tongji University, Shanghai, China, 200092*
[(3)] *Professor, Research Institute of Structural Engineering and Disaster Reduction, Tongji University, Shanghai, China, 200092*

Abstract

An interstory drift estimation method using structural acceleration measurements is firstly presented in this study. In this method, a six story finite element reinforced concrete model with concentrated plastic hinges, is decomposed into a series of single-degree-freedom substructures for interstory drift prediction. A virtual linear structural model, representing the linear behavior of the designed substructure, is utilized to generate reference response signals to obtain the tracking error of acceleration. The tracking error of displacement is subsequently estimated with the implementation of unbiased Kalman filtering approach, and the corresponding interstory drift of the objective substructure is then predicted accordingly. Four different noise conditions with signal-to-noise ratio of 20dB, 30dB, 40dB and 60dB are considered in the parametric study and the prediction performance of interstory drift, in terms of peak drift and time history, is investigated.

Keywords: Structural dynamics; Building structures; Interstory drift; Health monitoring; Earthquake

1. Introduction

Vibration-based non-destructive structural damage detection methods are essential and meaningful according to the purposes of evaluating health state of structures after severe disasters, such as earthquake, hurricane, tsunami and others. In the context of seismic-excited structures, strong hysteretic behaviors may be experienced and defined as the damage of structures, which are usually represented as the opening or close of cracks, yielding or buckling of material and the strength or stiffness degradation of structural members[1]. The correlation between a macroscopic physical parameter, such as interstory drift ratio (IDR), and the damage severity of a structure with hysteretic behaviors has been well recognized[2] and the implementation of such structural quantities of interests (drifts, forces, and energies) for seismic assessment can be found in several representative studies utilizing numerical models [3] and full-scale shaking table testing [4].

As the importance of interstory drift, several methods and techniques are investigated and developed aiming at the measuring structural displacement, such as the acceleration based approach, the global positioning systems (GPS) and vision-based method. In general, each of these methods has its feasibilities and limitations. The numerical method utilizing acceleration data with double integration procedure is widely known and utilized[5], while the acceleration data contaminated by measurement noise usually results in a existence of drift baseline, and a utilization of band-pass filter induces an unreliable displacement estimation of a nonlinear structure[6]. The state-of-the-art of GPS technologies in the field of high-rise building health monitoring since 1995 is discussed by Yi et al.[7] and the high-cost of this technology limits its applications. The video camera approach requires additional computational image processing which is not suitable for practical use neither[8]. Consequently, it is strongly desired to develop a general acceleration-based methodology for the nonlinear displacement estimation by the direct use of structural dynamic response measurements.

Alternative from signal processing, the estimation of structural displacement from acceleration can be recognized as a state identification problem in structural control area, which is predicting unknown system responses from available system outputs. For example, the most pronounced state observer is the Kalman filter for linear quadratic Gaussian (LQG) control on linear structures[9]. Currently, there are relatively fewer state estimators developed for nonlinear system than that for linear cases. Li et al. [10] pointed out that one of the existing problems for nonlinear estimator is the assumption of prior knowledge on nonlinear model structure with model parameters unknown. The state estimator for nonlinear system, with little prior or explicit knowledge of structural hysteretic behavior, appears to be a promising approach for interstory drift monitoring in near real-time during seismic events.

In this paper, a model-reference state observation procedure is proposed for nonlinear structural interstory drift estimation. The decomposition of the multiple degree-of-freedom structure (MDOF) into a series of single degree-of-freedom (SDOF) structures and the unbiased Kalman filter technology are adopted in the establishment of the state estimator. A six floor reinforced concrete frame model with concentrated plastic hinges, mimicked in Sap2000, is illustrated as the numerical example and the prediction performance of interstory drift, in terms of peak drift and time history, is investigated. To further discuss the robustness of the proposed method, a parametric study about signal-to-noise ratio (SNR) is demonstrated.

2. Formulation

A multi-story building structure can commonly be modeled in extreme simplicity as a shear beam structure. The governing equation of such structure with the hysteretic behavior subject to earthquake excitations can be written as

$$\mathbf{M}\ddot{\mathbf{x}} + \mathbf{C}\dot{\mathbf{x}} + \mathbf{F}(\mathbf{x}, \dot{\mathbf{x}}) = -\mathbf{M}\mathbf{h}\ddot{x}_g \tag{1}$$

where $\mathbf{x}$, $\dot{\mathbf{x}}$ and $\ddot{\mathbf{x}}$ denotes the relative displacement, velocity, and acceleration vectors, respectively; $\mathbf{F}$ is the nonlinear restoring force vector in a function of the response states $\mathbf{x}$ and $\dot{\mathbf{x}}$; $\mathbf{M}$ and $\mathbf{C}$ denote mass and damping matrices of the structure, respectively; $\ddot{x}_g$ is an excitation scalar representing ground acceleration distributed by the influence vector $\mathbf{h}$.

With the adoption of the Bouc-Wen model[11,12], which is used for analytically simulating the structural hysteresis at story-levels, the restoring force component f_i on the i th story can be represented as

$$f_i = \alpha_i k_i Y_i + (1-\alpha_i) k_i D_{y,i} z_i \tag{2}$$

where the subscript letter i refers to the story number of the corresponding matrices or vectors; α, k, and D_y are the ratio of post-yield, the pre-yield stiffness, and the yield deformation, respectively; z is the hysteretic component; Y is the interstory drift of the corresponding floor;

Eq. (1) and (2) describe a multiple degrees-of-freedom (MDOF) nonlinear structure, and consist of a series of differential equations, which can be written generally as Eq. (3) and (4) for seismic excitations from the force equilibrium consideration.

$$\begin{gathered} m_i \ddot{Y}_i + c_i \dot{Y}_i + \alpha_i k_i Y_i + (1-\alpha_i) k_i D_{y,i} z_i = p_i,\ i = 2 \cdots N \\ p_i = -\sum_{j=i+1}^{N} m_j \left(\ddot{x}_j + \ddot{x}_g \right) - m_i \left(\ddot{x}_{i-1} + \ddot{x}_g \right) \end{gathered} \tag{3}$$

$$\begin{gathered} m_1 \ddot{Y}_1 + c_1 \dot{Y}_1 + \alpha_1 k_1 Y_1 + (1-\alpha_1) k_1 D_{y,1} z_1 = p_1 \\ p_1 = - m_1 \ddot{x}_g - \sum_{j=2}^{N} m_j \left(\ddot{x}_j + \ddot{x}_g \right) \end{gathered} \tag{4}$$

For interstory drift estimation, it is necessary to construct a virtual linear system subject to the same input excitation p_i as a reference model for comparison. The dynamic equation for this reference linear system can be expressed directly as

$$m_i \ddot{Y}_i^r + c_i \dot{Y}_i^r + k_i Y_i^r = p_i,\ i = 1 \sim N \tag{5}$$

where Y_i^r indicates the interstory drift of the i th story of the virtual healthy system. As shown in Eq. (3) and (4), the external exciting force p_i can be directly obtained based on the ground and structural acceleration monitoring, and further be utilized to generate the desired response signal.

Subtracting Eq. (5) from Eq. (3) and (4), the following equation corresponding to a linear system can be established:

$$m_i \ddot{r}_i + c_i \dot{r}_i + k_i r_i = (1-\alpha_i) k_i \left(D_{y,i} z_i - Y_i \right),\ i = 1 \sim N \tag{6a}$$

$$\ddot{r}_i = \ddot{Y}_i^r - \ddot{Y}_i \tag{6b}$$

As can be seen in Eq. (6a), the terms on left side represent the linear status of the designated i th substructure and the right term represents the nonlinear hysteretic behavior which is usually unobservable in practice. The problem of obtaining the interstory drift turns out to be a problem of state observation without input information in a designed linear system. The state space description is adopted here for Eq. (6a), and a three-step recursive filter with minimum-variance unbiased characteristics [13] is utilized to estimate the state vector $\mathbf{z}_i = [r_i, \dot{r}_i]^T$ with the unknown disturbance $d_i = (1-\alpha_i) k_i \left(D_{y,i} z_i - Y_i \right)$.

The equation of the unbiased Kalman filtering approach for the discrete time state-space model is then summarized briefly as follows[**¡Error! Marcador no definido.**]

Step 1: Initialization

$$j = 0,\ \hat{z}_{0/0} = \overline{z}_0,\ \hat{d}_0 = \overline{d}_0,\ P_{0/0}^z = P_0 \tag{7}$$

Step 2: Time Update

$$\begin{aligned}
&\hat{z}_{j+1/j} = A\hat{z}_{j/j} + B\hat{d}_j \\
&P^z_{j+1/j} = [A,B]\begin{bmatrix} P^z_{j/j} & P^{zd}_j \\ P^{dz}_j & P^d_j \end{bmatrix}\begin{bmatrix} A^T \\ B^T \end{bmatrix} + Q
\end{aligned} \tag{8}$$

Step 3: Estimation of unknown input (disturbance)

$$\begin{aligned}
&\tilde{R}_{j+1} = CP^z_{j+1/j}C^T + R \\
&N_{j+1} = \left(D^T\tilde{R}^{-1}_{j+1}D\right)^{-1}D^T\tilde{R}^{-1}_{j+1} \\
&\hat{d}_{j+1} = N_{j+1}\left(y_{j+1} - C\hat{z}_{j+1/j}\right) \\
&P^d_{j+1} = \left(D^T\tilde{R}^{-1}_{j+1}D\right)^{-1}
\end{aligned} \tag{9}$$

Step 4: Measurement update

$$\begin{aligned}
&G_{j+1} = P^z_{j+1/j}C^T\tilde{R}^{-1}_{j+1} \\
&\hat{z}_{j+1/j+1} = \hat{z}_{j+1/j} + G_{j+1}\left(y_{j+1} - C\hat{z}_{j+1/j} - D\hat{d}_{j+1}\right) \\
&P^z_{j+1/j+1} = P^z_{j+1/j} - G_{j+1}\left(\tilde{R}_{j+1} - DP^d_{j+1}D^T\right)G^T_{j+1} \\
&P^{zd}_{j+1} = \left(P^{dz}_{j+1}\right)^T = -G_{j+1}DP^d_{j+1}
\end{aligned} \tag{10}$$

Step 5: $j = j+1$ and return to Step 2.

where A, B, C, and D are the matrices of the discrete time state-space model, Q, R, $P^z_{j/j}$, P^d_j, P^{dz}_j and P^{zd}_j are the covariance matrices, $\tilde{R}^{-1}_j$ and G_j are the weighting matrices; and N_j is the optimal matrix.

3. Numerical simulation

The model considered herein is a six floor finite element reinforced concrete frame structure, as illustrated in Fig.1, which is mostly referred to the model setups by Alhaddad et al. [14]. The story height of the designated model was 3.2 m and the span width is 6.0 m in both directions. Material properties were assumed to be 28 MPa for concrete compressive strength and 420 MPa for yielding strength of both longitudinal and transverse reinforcement. The cross sections of columns and beams were and mm, respectively, and the thickness of slabs was 250 mm. Gravity loads were $8.5\,\mathrm{kN/m^2}$ and $1.5\,\mathrm{kN/m^2}$ for dead and live loads, respectively. The nonlinear behavior was simulated by the plastic hinge models of P-M2-M3 and M3 hinges distributed at the end of column and beam elements, respectively. The nonlinear response history analysis is performed on the platform of SAP2000.

Three earthquake records, the 1940 Imperial Valley earthquake recorded at El Centro station, the 1994 Northridge earthquake recorded at Sylmar station, and the 1995 Kobe earthquake recorded at KJMA station, were used as excitation sources to the present FE model, as listed in Table 1. Five excitation scenarios are considered herein for the performance study of proposed interstory drift estimation method. Firstly, the 1994 Northridge and the 1995 Kobe earthquake records with PGA of $1\,\mathrm{m/s^2}$ were assigned as Case I and II, respectively. Secondly, the 1994 Northridge, the 1995 Kobe and the 1940 El Centro records with PGA of 2, 4 and 6 $\mathrm{m/s^2}$ were then assumed as Case III, IV and V, respectively. The five excitation cases were unidirectional excitations in the one-bay transverse direction. The absolute acceleration response of all floors were measured and utilized in both system simplification and interstory drift estimation. The sampling frequency of the data was 1,000 Hz, and the measurement noise was assumed with a signal-to-noise ratio of 60dB, 40dB, 30 dB and 20dB.

For the adopted method, the constant covariance matrices Q and R of the adopted unbiased Kalman filter and the initial values of matrices P_0, P_0^d, P_0^{dz} and P_0^{zd} were defined as

$$Q=\begin{bmatrix}0.05 & 0\\ 0 & 0.05\end{bmatrix},\ R=0.1,\ P_0=\begin{bmatrix}20 & 0\\ 0 & 20\end{bmatrix},\quad P_0^d=20,\quad P_0^{zd}=\left(P_0^{dz}\right)^{\mathrm{T}}=\begin{bmatrix}0\\0\end{bmatrix} \tag{11}$$

The initial condition of state estimation $\bar{z}_0$ and the unknown disturbance $\bar{d}_0$ was assigned as zero. The calculated tracking error of acceleration $\dot{r}$ was firstly calculated with the generated reference signals from the prior-constructed linear model. The state estimation was subsequently carried out with a time interval of 0.0005 second. The decrease of time interval of the tracking error signal was performed utilizing a piecewise cubic interpolation technique.

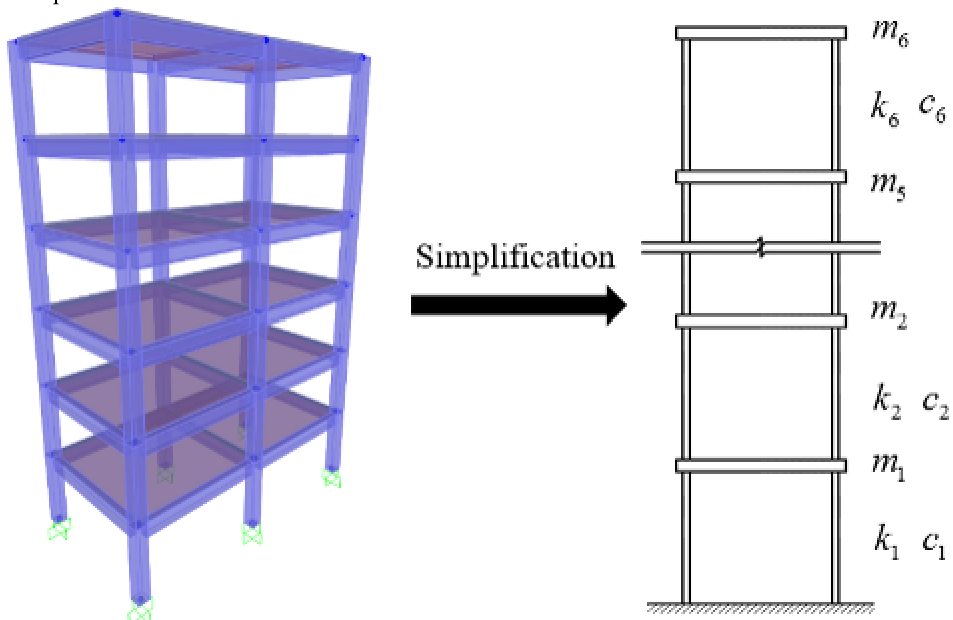

Fig. 1 – Six-story finite element frame model and the corresponding simplified shear-type model

Table 1 – Basic information of selected ground motions for numerical analysis

Earthquake	Year	Station	Magnitude	PGA (g)
Imperial Valley	May 19, 1940	El Centro	7.10	0.35
Northridge	January 17, 1994	Sylmar-Olive View Med FF	6.69	0.84
Kobe	January 16, 1995	KJMA	6.90	0.83

For the present assessment method, a reduced-order shear-type model was introduced to represent the linear behavior of the numerical model in Case I and II, and was further used as the reference model in Case III~V. According to the accelerometer placement, the condensed linear model with the monitored DOFs preserved presents six subspaces for the six-story FE model. Each floor from the first floor to the sixth floor composed a separated monitoring area, for example Substructure I corresponds to the first floor. The mass of each substructure was lumped and determined equally as 72948 kg. The interstory damping and stiffness coefficients were then identified utilizing the differential evolution (DE) algorithm. The damping and stiffness coefficients, using the acceleration measurements from Case I, were identified as $[1.485, 1.456, 1.401, 1.424, 1.444, 1.444]\times10^6$ N-s/m and $[1.521, 1.461, 1.460, 1.443, 1.454, 1.458]\times10^8$ N/m from first floors to sixth floors, respectively. Fig.2 shows the absolute acceleration responses between the numerical simulation and the state observer of first, third and fifth floor in Case I and II. Excellent correlations between the measurements and calculations of the absolute accelerations were illustrated both in the estimation scenario (Case I) and the validation scenario (Case II), which indicates the feasible representation of the linear behavior of the complex FE model.

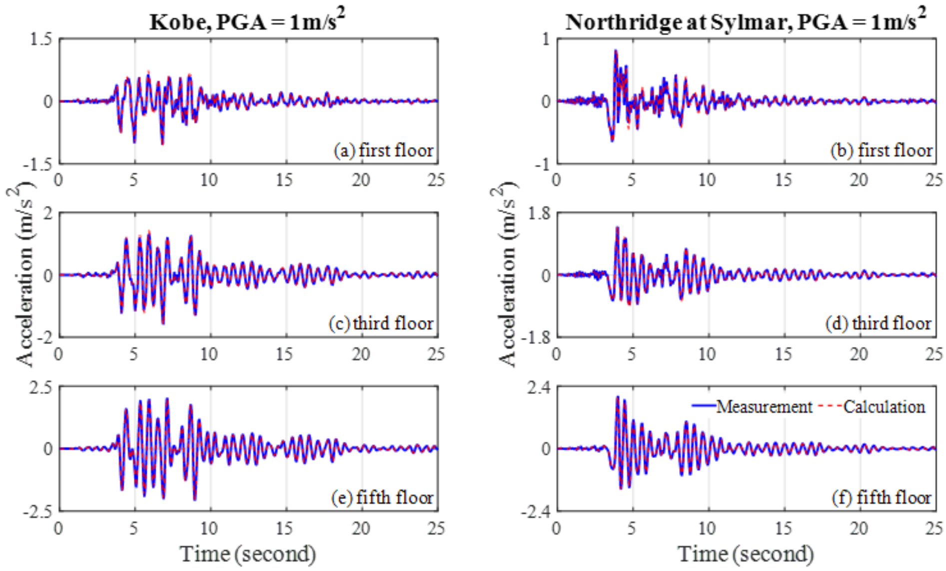

Fig. 2 – Comparison of the acceleration responses between the finite element model and the identified shear-type model: (a), (c) and (e) are for Case I; and (b), (d) and (f) are for Case II

The developments of structural hysteretic behavior of the first and sixth floor subjected to scenario V with signal-to-noise ratio of 20dB acceleration measurements were presented in Fig.3 (a) and (c) and corresponding interstory drift time history were presented in Fig.3 (b) and (d). Comparing to the sixth floor with less damage, severe hysteretic behavior presented in the first floor with an explicit residual drift phenomenon is observed. The interstory drift time history estimation utilizing double integration method of first and sixth floors subjected to scenario V were illustrated in Fig.3 (b) and (d), respectively. As can be seen in Fig.3 (b), the double integration method cannot predict nonlinear displacement accurately and the residual drift was removed owing to the band-pass filtering procedure. Moreover, in Fig.3 (d), the noise in measured signal will also influence the prediction accuracy of displacement estimation.

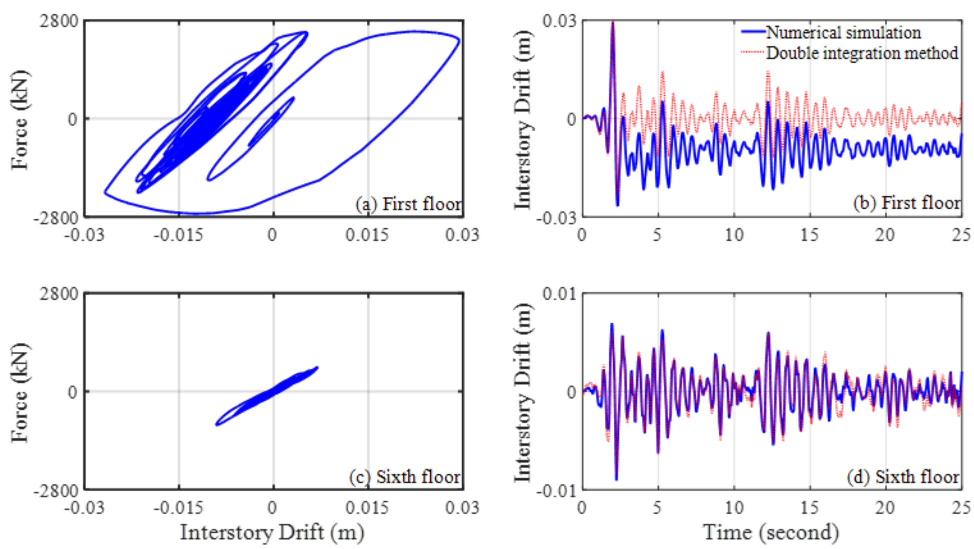

Fig. 3 – The development of structural hysteretic behavior and the time history of interstory drift of first and sixth floors subject to scenario V with noise-polluted acceleration measurement condition

Fig.4 compares of the interstory drift time history of first and sixth floors subjected to Case V with a signal-to-noise ratio of 30 dB and 20dB. As can be seen in Fig.4 (c) and (d), a favorable prediction of interstory drift is observed with different noise level, and the root-mean-square (RMS) error of the estimated interstory drift was as 11.16% in the case with SNR as 20dB, illustrated in Fig.4 (d), which is nearly a quarter of the root-mean-square error of prediction utilizing double integration method as 42.46%, shown in Fig.3 (d). Unlike the favorable prediction performance in Fig.4 (c) and (d), there exists a noticeable underestimation of baseline shift of raw estimation of interstory drift illustrated in Fig.4 (a) and (b), especially in the last part of the responses. At this circumstance, a correction method, as to improve the performance of raw estimation of interstory drift, is subsequently proposed.

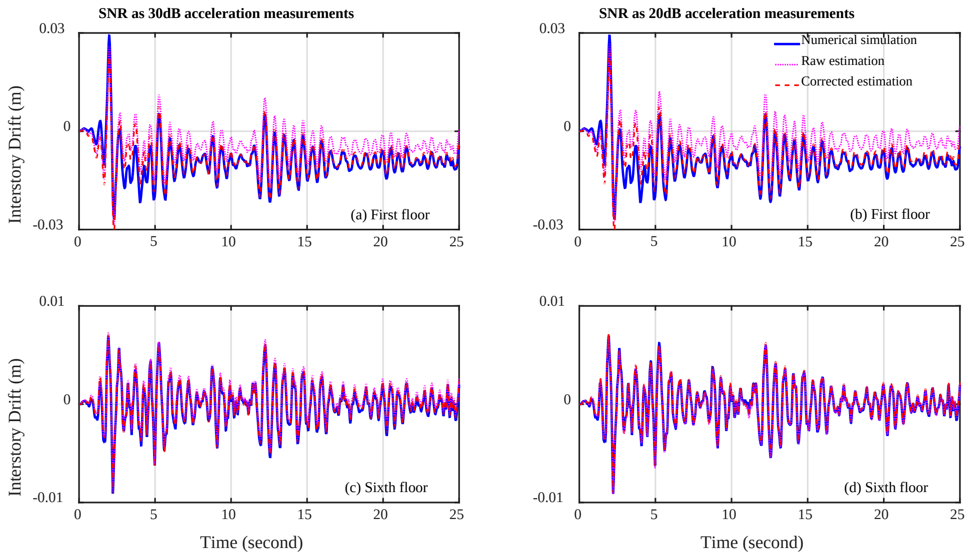

Fig. 4 – Comparison of the interstory drift time history of first and sixth floors subjected to scenario V with different noise-polluted measurement condition

In order to improve the performance of the unbiased Kalman filter on the state estimation and simultaneously preserve the valuable information of the overall residual displacement, several steps are further performed to correct the raw estimate: (1) obtain a polynomial $L(t)$ fitting the overall disturbance estimate $\hat{d}(t)$ in the least square sense; (2) assume an optimal weight factor μ to scale the preliminary polynomial $L(t)$; (3) calculate the interstory drift responses with a new disturbance $\hat{d}(t)-\mu L(t)$ using the model described in Eq. (6); (4) determine the optimal weight factor μ_{opt} that presents the closest match of the ending residual drift between the corrected estimation and the prior-known measurement. And a remarkable improvement of interstory drift as compared to raw estimation is observed in Fig.4 (a) and (b).

$$J_{d,i}^{r}=\frac{\mathbf{rms}\left(\mathbf{y}_{d,i}-\hat{\mathbf{y}}_{d,i}\right)}{\mathbf{rms}\left(\mathbf{y}_{d,i}\right)}$$
$$J_{d,i}^{p}=\frac{\left|\mathbf{max}\left(\left|\mathbf{y}_{d,i}\right|\right)-\mathbf{max}\left(\left|\hat{\mathbf{y}}_{d,i}\right|\right)\right|}{\mathbf{max}\left(\left|\mathbf{y}_{d,i}\right|\right)} \tag{12}$$

where $\mathbf{rms}$ is the root-mean-square operator; $\mathbf{max}$ denotes the largest element in the array; $\mathbf{y}_{d,i}$ and $\hat{\mathbf{y}}_{d,i}$ are the reference and estimated interstory drift time history of i th floor, respectively; $J_{d,i}^{r}$ and $J_{d,i}^{p}$ indicate the discrepancy of RMS value and peak drift value of i th floor, respectively; the subscript d denotes displacement.

According to the Eq. (12), Fig.5 compares the discrepancy of peak drift value and RMS value subjected to scenarios I to V with the same acceleration measurement condition of SNR as 20dB. Firstly, linear scenarios I and II were depicted as reference of the discrepancy of peak drift value and RMS value between the response of identified shear-type model and response from Sap2000 simulation. Secondly, nonlinear scenarios III to V were depicted as the discrepancy of peak drift value and RMS value between the response estimated by the proposed interstory drift estimation method and response from Sap2000 simulation. The structural realization as the identified shear-type model, subjected to case I and II with SNR as 20dB, shows a remarkable response discrepancy probably induced by a combined influence of model simplification and measured noise. The discrepancy of peak value and RMS value, in the nonlinear scenarios, are bounded between 0.1%~9.6% and 6.15%~29.02%, respectively. Furthermore, comparing linear cases (I and II) and nonlinear cases (III, IV and V), it seems the proposed interstory drift estimation method have a favorable prediction performance as it had a lower discrepancy level, except the second floor.

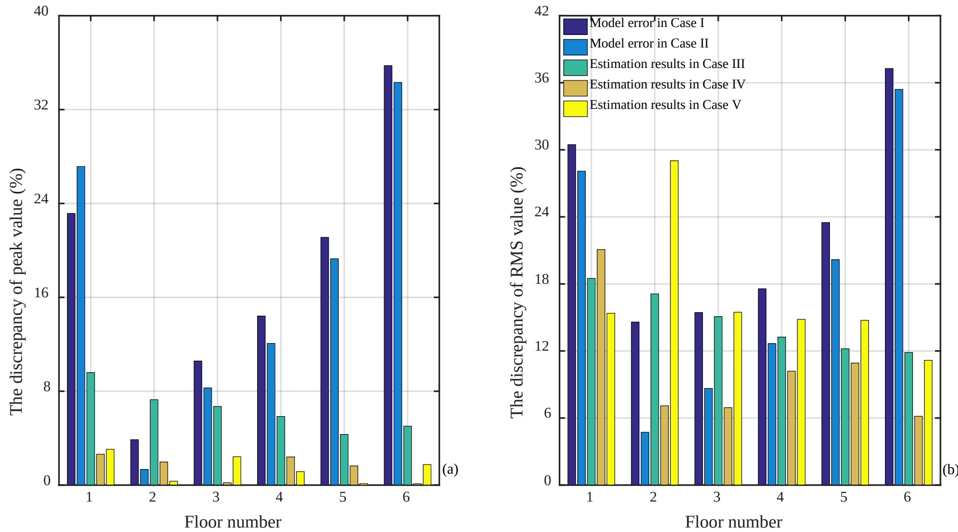

Fig. 5 – The comparison of estimation discrepancies of peak drift value and RMS value subjected to five scenarios

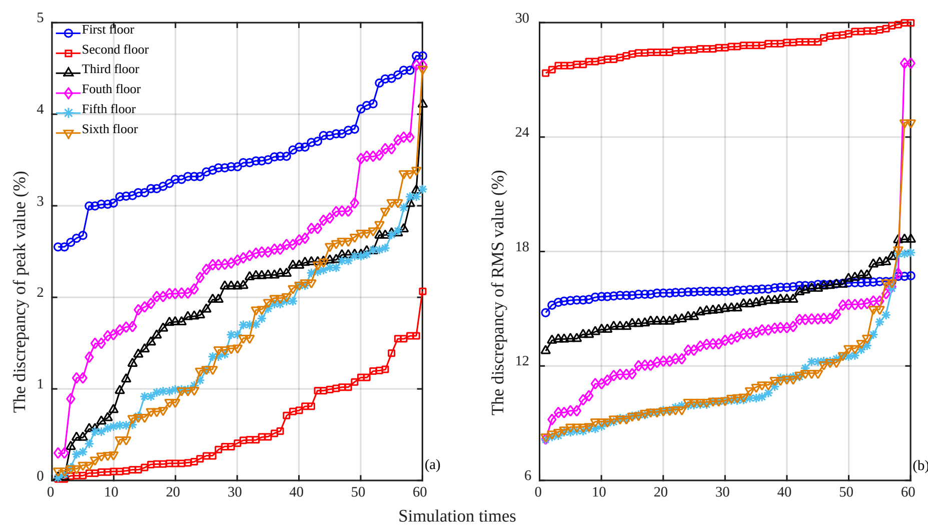

Fig. 6 – The influence of measurement noise to the robustness of proposed interstory drift estimation method

To investigate the influence of unpredictable noise to the robustness of the proposed method, the discrepancy of peak value and RMS value of a series of independent simulations, subjected to El Centro earthquake with PGA as 6 m/s^2 and SNR as 20dB, were illustrated in Fig.6 (a) and (b), respectively. Fig.6 (a) indicates the discrepancy of estimated peak value are bounded between 0.01% and 4.64% and Fig.6 (b) indicates the discrepancy of estimated RMS value are bounded between 8.14% and 29.99%. The further statistic values of the discrepancy results, such as mean value and the standard deviation value, were listed in Table 2. As can be seen, the standard deviation values of the discrepancy of peak value and RMS value are smaller than 1.07% and 3.30%, respectively, which spells out the stable performance of the proposed method in most simulation cases. And the average extend of the discrepancy among six floors of the sixty simulations are represented as the mean value with the maximum mean discrepancy of peak value of 3.51% in the first floor and the maximum mean discrepancy of RMS value of 28.73% in the second floor. These statistic values, on the other hand, indicate the reliability of the results illustrated in Fig.5.

Table 2 – Statistic results of the discrepancy of peak value and RMS value under sixty individual simulation cases subjected to El Centro earthquake with SNR as 20dB

Floor	Discrepancy of peak value (%)		Discrepancy of RMS value (%)	
	Mean	Standard deviation	Mean	Standard deviation
Floor 1	3.51	0.52	15.96	0.38
Floor 2	0.58	0.51	28.73	0.64
Floor 3	1.90	0.82	15.23	1.40
Floor 4	2.42	0.89	13.50	3.30
Floor 5	1.57	0.87	10.94	2.35
Floor 6	1.61	1.07	11.32	3.26

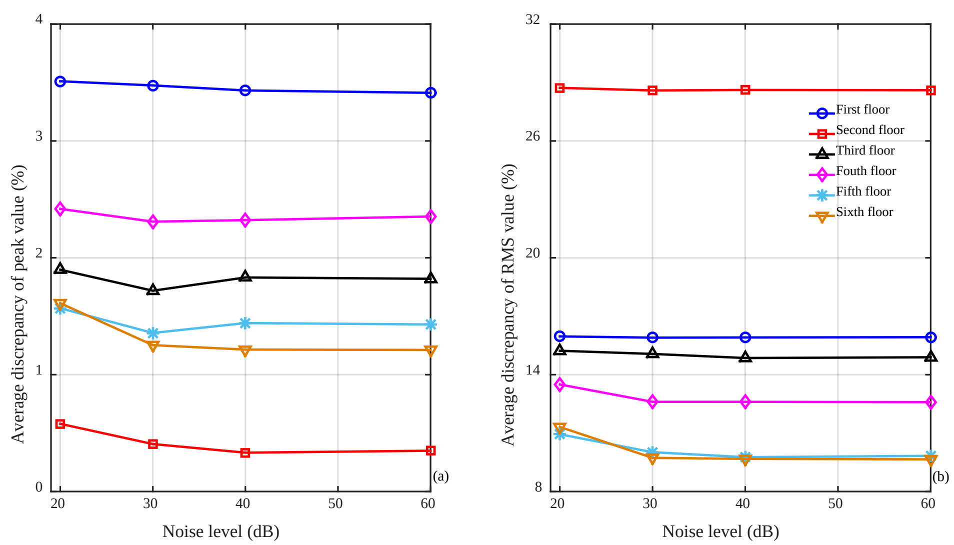

Fig. 7 – The comparison of average discrepancy of peak and RMS value subjected to El Centro earthquake with different noise level scenarios

As illustrated in Fig.7, the average discrepancy of peak and RMS value subjected to El Centro earthquake with different noise level scenarios shows a stable performance of the proposed interstory drift estimation method. The average discrepancy of peak value of the first floor are bounded between 3.41% and 3.51%, and the average discrepancy of RMS value of the second floor are bounded between 28.61% and 28.73%, which indicate the influence of noise to the proposed estimation method are small as the noise level grows and the residual estimation error seems to stemming from the influence of model error and seismic characteristics. The average discrepancy of peak value of the second floor are bounded between 0.33% and 0.58%, and the average discrepancy of RMS value of the second floor are bounded between 9.65% and 11.32%, which indicate the influence of noise to the proposed estimation method increases as the discrepancy level decreases.

4. Conclusion

An interstory drift estimation method for seismic-excited building structure was presented in this study. The Bouc-Wen model was only used to represent the nonlinear hysterestic structural behavior to stimulate structural acceleration data. Besides, the reference model, which is free of the prior knowledge of hysteretic models, was obtained in the light of a story-level physics-based structural identification method. A decomposition process to the MDOF system and an unbiased Kalman filter were integrated in the proposed algorithm. One six story finite element model with concentrated plastic hinges are utilized for the numerical investigation of the present algorithm, with the prediction performance evaluated in both peak drift and time history. The predicted results are numerically demonstrated with favorable agreement to the actual interstory drift responses.

5. Acknowledgements

This study is sponsored by the National Science Foundation of China (Grant No: 51408435) and the Fundamental Research Funds for the Central Universities.

6. Copyrights

7. References

[1] Loh, C. H., Mao, C. H., Huang, J. R., Pan, T. C. (2011): System identification and damage evaluation of degrading hysteresis of reinforced concrete frames. *Earthquake Engineering & Structural Dynamics*, **40** (6), 623-640.

[2] Shodja, A. H., Rofooei, F. R. (2014). Using a lumped mass, nonuniform stiffness beam model to obtain the interstory drift spectra. *Journal of Structural Engineering*, **140** (5), 04013109.

[3] Ghosh, S., Datta, D., Katakdhond, A. A. (2011). Estimation of the Park–Ang damage index for planar multi-storey frames using equivalent single-degree systems. *Engineering Structures*, **33** (9), 2509-2524.

[4] Ceccotti, A., Sandhaas, C., Okabe, M., Yasumura, M., Minowa, C., Kawai, N. (2013). SOFIE project-3D shaking table test on a seven-storey full-scale cross-laminated timber building. *Earthquake Engineering & Structural Dynamics*, **42** (13), 2003-2021.

[5] Çelebi, M. (2008). Real-time monitoring of drift for occupancy resumption. *14th World Conference on Earthquake Engineering 14WCEE*, Beijing, China.

[6] Skolnik, D. A., Wallace, J. W. (2010). Critical assessment of interstory drift measurements. *Journal of Structural Engineering*, **136** (12), 1574-1584.

[7] Yi, T. H., Li, H. N., Gu, M. (2013). Recent research and applications of GPS-based monitoring technology for high-rise structures. *Structural Control and Health Monitoring*, **20** (5), 649-670.

[8] Matsuya, I., Katamura, R., Sato, M., Iba, M., Kondo, H., Kanekawa, K., Shoji, S. (2010). Measuring relative-story displacement and local inclination angle using multiple position-sensitive detectors. *Sensors*, **10** (11), 9687-9697.

[9] Wu, J. C., Yang, J. N. (2000). LQG control of lateral–torsional motion of Nanjing TV transmission tower. *Earthquake Engineering & Structural Dynamics*, **29** (8), 1111-1130.

[10] Li, H., Mao, C. X., Ou, J. P. (2012). Identification of hysteretic dynamic systems by using hybrid extended Kalman filter and wavelet multiresolution analysis with limited observation. *Journal of Engineering Mechanics*, **139** (5), 547-558.

[11] Wen, Y. K. (1976). Method for random vibration of hysteretic systems. *Journal of the Engineering Mechanics Division*, **102** (2), 249-263.

[12] Pan, T. C., Lee, C. L. (2002). Application of wavelet theory to identify yielding in seismic response of bi-linear structures. *Earthquake Engineering & Structural Dynamics,* **31** (2), 379-398.

[13] Gillijns, S., De Moor, B. (2007). Unbiased minimum-variance input and state estimation for linear discrete-time systems with direct feedthrough. *Automatica*, **43** (5), 934-937.

[14] Alhaddad, M. S., Wazira, K. M., Al-Salloum, Y. A., Abbas, H. (2015). Ductility damage indices based on seismic performance of RC frames. *Soil Dynamics and Earthquake Engineering*, **77**, 226-237.